Original Article

A bioinformatics analysis of the PIEZO channel interaction network and the genes related to glycometabolic reprogramming and mitochondrial oxidative phosphorylation in the progression of prostatic hyperplasia

Yajie Zheng[1#], Fuguang Zhao[2,3#], Pengwei Xu[4], Chuchu Zeng[1], Zongrun Sun[1], Guanlin Wu[5], Yibin Wang[1]

[1]Department of Urology, Tongren Hospital, Shanghai Jiao Tong University School of Medicine, Shanghai, China; [2]Department of Urology, The Third Medical Center, Chinese People's Liberation Army (PLA) General Hospital, Beijing, China; [3]Department of Urology, The Seventh Medical Center, Chinese People's Liberation Army (PLA) General Hospital, Beijing, China; [4]Department of Urology, Suzhou Ninth People's Hospital, Suzhou Ninth Hospital Affiliated to Soochow University, Suzhou, China; [5]School of Clinical Medicine, Shanghai University of Medicine & Health Sciences, Shanghai, China

Contributions: (I) Conception and design: Y Wang, G Wu; (II) Administrative support: C Zeng, Z Sun; (III) Provision of study materials or patients: P Xu; (IV) Collection and assembly of data: F Zhao, Y Zheng; (V) Data analysis and interpretation: F Zhao, Y Zheng; (VI) Manuscript writing: All authors; (VII) Final approval of manuscript: All authors.

[#]These authors contributed equally to this work.

Correspondence to: Guanlin Wu, MD. School of Clinical Medicine, Shanghai University of Medicine & Health Sciences, No. 279 Zhouzhu Road, Pudong New Area, Shanghai 201318, China. Email: wugl@sumhs.edu.cn; Yibin Wang, MD. Department of Urology, Tongren Hospital, Shanghai Jiao Tong University School of Medicine, No. 1111 Xianxia Road, Changning Area, Shanghai 200336, China. Email: dryibinw@163.com.

Background: Prostatic hyperplasia is a common condition among aging males characterized by excessive prostate cell proliferation, and while it is a benign process, it involves significant metabolic reprogramming and immune infiltration—features typically associated with malignant tumors. This study aimed to elucidate the interaction network between the PIEZO channels and genes related to glycometabolic reprogramming and mitochondrial oxidative phosphorylation (OXPHOS), highlighting their roles in the progression of prostatic hyperplasia.

Methods: Gene expression datasets from the National Center for Biotechnology Information (NCBI) Gene Expression Omnibus (GEO) database were analyzed to identify differentially expressed genes (DEGs) associated with prostatic hyperplasia. Glycolysis- and OXPHOS-related pathways were obtained from the Molecular Signatures Database (MSigDB). Advanced bioinformatics methods, including differential expression analysis, functional enrichment analysis, immune infiltration analysis, and machine learning models, were employed to explore PIEZO interactions. A competitive endogenous RNA (ceRNA) network and a biomarker-based diagnostic nomogram were constructed and validated across multiple datasets.

Results: A total of 4,617 DEGs were identified, among which 122 were glycolysis- and OXPHOS-related genes. The Spearman correlation analysis revealed 84 genes significantly associated with PIEZO1 and PIEZO2 expression. The functional enrichment analysis demonstrated that these PIEZO-related genes regulate critical processes, including ATP production, mitochondrial function, and glycolysis. The immune infiltration analysis revealed associations between PIEZO biomarkers and altered immune cell profiles. Machine learning models identified PGM2 and GFPT1 as robust diagnostic biomarkers with strong predictive performance [area under the curve (AUC) >0.75]. The ceRNA network revealed complex regulatory interactions involving PIEZO genes, biomarkers, microRNAs (miRNAs), and long non-coding RNAs (lncRNAs), underscoring their potential roles in disease pathogenesis.

Conclusions: This study provides a comprehensive bioinformatics framework linking PIEZO channels to glycometabolic reprogramming and OXPHOS dysregulation in prostatic hyperplasia. The identified

biomarkers and regulatory networks offer novel insights into the molecular mechanisms underlying disease progression and potential therapeutic targets.

Keywords: Prostatic hyperplasia; PIEZO channels; glycometabolic reprogramming; mitochondrial oxidative phosphorylation (mitochondrial OXPHOS); biomarkers

Submitted Jan 22, 2026. Accepted for publication Feb 27, 2026. Published online Mar 23, 2026.
doi: 10.21037/tau-2026-1-0075
View this article at: https://dx.doi.org/10.21037/tau-2026-1-0075

Introduction

Prostatic hyperplasia, a prevalent condition among aging males, is characterized by the abnormal growth of the prostate gland, resulting in significant morbidity due to urinary obstruction and related complications (1). Despite substantial progress in understanding the clinical and pathological features of this disease, the underlying molecular mechanisms remain incompletely elucidated, hindering the development of effective therapeutic strategies (2). Recent advances in bioinformatics and molecular biology have enabled the exploration of complex gene networks and their roles in disease pathogenesis, providing novel insights into metabolic and cellular dysfunctions (3,4).

Mechanotransduction, mediated by PIEZO ion channels (PIEZO1 and PIEZO2), has emerged as a critical regulator of cellular physiology, particularly in the context of mechanical stress and tissue remodeling (5). PIEZO channels are mechanosensitive ion channels that translate physical forces into biochemical signals, influencing various cellular processes, including proliferation, apoptosis, and metabolism (6). Notably, growing evidence links PIEZO channels to metabolic reprogramming—a hallmark of numerous hyperplastic and neoplastic conditions (7). Mechanosensation via PIEZO channels can alter glycolysis and mitochondrial oxidative phosphorylation (OXPHOS), two key metabolic pathways implicated in cellular energy production and biosynthesis. These alterations may underpin the pathological growth observed in hyperplastic prostate tissues, providing a potential mechanistic link between mechanical stimuli and metabolic dysregulation.

Glycometabolic reprogramming, which involves alterations in glycolysis and mitochondrial activity, has been recognized as a key driver of cellular proliferation in prostatic hyperplasia (8). The metabolic demands of hyperplastic tissues necessitate the dynamic reorganization of energy production pathways, favoring processes such as aerobic glycolysis (the Warburg effect) and altered mitochondrial respiration (9,10). PIEZO-mediated calcium signaling is thought to play a pivotal role in orchestrating these metabolic shifts, thereby linking mechanotransduction to metabolic regulation. However, little is known about the interaction networks between PIEZO channels and metabolic pathways in the context of prostatic hyperplasia.

This study aimed to elucidate the molecular interplay

Highlight box

Key findings

- This study showed that PIEZO channels are significantly associated with genes related to glycometabolic reprogramming and mitochondrial oxidative phosphorylation (OXPHOS) in prostatic hyperplasia, with 84 genes strongly correlated with PIEZO1/2. Two key biomarkers, PGM2 and GFPT1, were shown to be robust diagnostic markers with high predictive accuracy across multiple datasets.

What is known, and what is new?

- Previous studies have shown that prostatic hyperplasia involves metabolic reprogramming and abnormal cell proliferation, and that PIEZO channels serve as mechanosensitive regulators involved in cellular metabolism and disease progression, including hyperplastic conditions.
- This study established a comprehensive bioinformatics framework linking PIEZO channels to specific metabolic pathways in prostatic hyperplasia, and identified and validated the performance of PGM2 and GFPT1 as novel diagnostic biomarkers. It also constructed a competitive endogenous RNA network, showing the post-transcriptional regulation of PIEZO genes.

What is the implication, and what should change now?

- The study findings imply that PIEZO-mediated metabolic dysregulation is a potential therapeutic target for prostatic hyperplasia. Future research should include the experimental validation of the PIEZO-metabolic interactions and the clinical application of the identified biomarkers for diagnosis and targeted therapy.

Table 1 The basic information of the datasets used in this study

ID	Data type	Platform	BPH	HC	Resource	Note
GSE132714	Microarray	GPL16791	18	4	Serum	Training set
GSE7307	Microarray	GPL570	7	13	Mucosa	Validation set
GSE6099	Microarray	GPL2013	11	23	Tissue	Validation set

BPH, benign prostatic hyperplasia; HC, healthy control.

between PIEZO ion channels and glycometabolic reprogramming in the progression of prostatic hyperplasia, using advanced bioinformatics approaches. Specifically, it sought to: identify key genes and pathways linking PIEZO channels to glycolysis and OXPHOS using publicly available gene expression datasets; explore the regulatory networks involving PIEZO channels, metabolic genes, and immune cell infiltration to determine their roles in the pathophysiology of prostatic hyperplasia; and validate the candidate biomarkers associated with PIEZO-mediated metabolic reprogramming and their diagnostic potential in distinguishing prostatic hyperplasia from normal tissues. By integrating differential gene expression analyses, pathway enrichment analyses, and machine learning approaches, this study aimed to construct a comprehensive interaction network that highlights the role of PIEZO channels in metabolic and immune dysregulation in prostatic hyperplasia. The study findings could pave the way for novel therapeutic targets and biomarker development, addressing the unmet clinical needs in managing this common but understudied condition. We present this article in accordance with the TRIPOD reporting checklist (available at https://tau.amegroups.com/article/view/10.21037/tau-2026-1-0075/rc).

Methods

Data acquisition

The study used publicly available gene expression datasets related to benign prostatic hyperplasia (BPH) from the National Center for Biotechnology Information (NCBI) Gene Expression Omnibus (GEO) database. Details of the datasets used are provided in *Table 1*. Moreover, gene sets related to glycolysis and OXPHOS were obtained from the Molecular Signatures Database (MSigDB). A total of 259 glycolysis-related genes were obtained from the HALLMARK_GLYCOLYSIS and REACTOME_GLYCOLYSIS pathways (version 2024.1). These pathways were selected based on their relevance to glycolytic processes (11). A total of 200 OXPHOS-related genes were obtained from the HALLMARK_OXIDATIVE_PHOSPHORYLATION pathway (version 2024.1). This pathway captures key processes involved in mitochondrial OXPHOS (12).

Differential expression analysis

To investigate the interaction between the PIEZO channels and genes related to glycometabolic reprogramming and mitochondrial OXPHOS in the progression of BPH, differentially expressed genes (DEGs) were identified between the BPH and control samples in the GSE132714 training dataset. The "limma" package in R was used for the differential analysis, following data normalization using the "normalizeBetweenArrays" function. The DEGs were selected using thresholds of a $|\log_2$ fold change (FC)$|$ >1 and a P value <0.05. The results were visualized in a volcano plot generated using the "ggplot2" package.

Validation of biomarker genes

To validate the biomarkers identified through machine learning, two independent validation datasets, GSE7307 and GSE6099, were analyzed alongside the training dataset, GSE132714. The preprocessing and normalization of all datasets were performed using the "normalizeBetweenArrays" function from the "limma" R package.

To confirm the differential expression of the key biomarkers between the BPH and normal samples, gene expression levels were compared across the training and validation datasets (GSE132714, GSE7307, and GSE6099). Wilcoxon tests were used for the statistical analysis, with a significance threshold of P<0.05.

Receiver operating characteristic (ROC) curve analysis

The diagnostic ability of the five candidate biomarkers identified from machine learning models was evaluated

using ROC curves in both the training and validation datasets. Genes with area under the curve (AUC) values greater than 0.75 were considered to have strong diagnostic potential. ROC curves were generated to visualize the performance of these biomarkers.

Functional enrichment analysis of candidate genes

The candidate genes were subjected to Gene Ontology (GO) and Kyoto Encyclopedia of Genes and Genomes (KEGG) pathway enrichment analyses using the "clusterProfiler" package in R. Functional enrichment analyses were performed for the biological processes (BPs), cellular components (CCs), and molecular functions (MFs), as well as the KEGG pathways, with results filtered at a P adjusted value <0.05. The top 10 terms or pathways were visualized as bubble plots, in which the bubble size indicates the number of enriched genes and color intensity reflects the statistical significance.

Immune cell infiltration analysis

To investigate immune cell infiltration in BPH, the CIBERSORT algorithm was applied to the training dataset to estimate the relative abundance of 22 immune cell types in the BPH and normal samples. Differences in immune cell composition between the two groups were assessed using the Wilcoxon rank-sum test. The proportions of immune cells were visualized using stacked bar plots generated with the "ggplot2" R package. The abundance of each of the 22 immune cell types was compared between the BPH and normal samples using the Wilcoxon test. The results were visualized in violin plots, indicating the statistical significance of the observed differences.

Statistical analysis

The Spearman correlation analysis revealed 84 DE-glycolysis-OXPHOS genes strongly associated with *PIEZO1* and *PIEZO2* expression (|Cor| >0.6, P<0.05). These PIEZO-related genes were visualized in heatmaps and correlation plots. To explore the relationships between the PIEZO-associated biomarkers and differentially abundant immune cells, a Spearman correlation analysis was performed using the "psych" R package. Correlations with |Cor| >0.3 and P<0.05 were considered significant, and the results were visualized in scatter plots.

Gene Set Enrichment Analysis (GSEA)

To further investigate the functional roles of the hub genes in distinguishing between the BPH and normal samples, a single-sample GSEA was performed using the "GSEA" R package. Correlations between each hub gene and all the other genes were calculated, ranked, and subjected to GSEA to identify enriched KEGG pathways. The top six enriched pathways for each diagnostic gene were visualized. The analysis followed the methodology described in an earlier study (13).

Gene Set Variation Analysis (GSVA)

To explore the pathway activation patterns associated with hub gene expression, a GSVA was conducted using the "GSVA" R package. Samples were grouped into high- and low-expression groups for each hub gene, and pathway enrichment was compared by differential analysis using the "limma" R package. Differentially activated pathways were identified using thresholds of |t| >2 and P<0.05. Pathways with t values >0 were considered high-expression pathways, and those with t values <0 were considered low-expression pathways. The results were visualized to highlight functional distinctions.

Construction of the competitive endogenous RNA (ceRNA) network

To explore the regulatory interactions involving the *PIEZO* genes (*PIEZO1* and *PIEZO2*) and biomarkers, the RNAInter database was used to identify lncRNA and miRNA interaction pairs with a score threshold >0.7. Identified interactions were integrated to construct a ceRNA network. The network was visualized using Cytoscape software, comprising nodes representing genes, long non-coding RNAs (lncRNAs), and microRNAs (miRNAs), along with edges denoting their interactions.

Construction of a nomogram for biomarker-based prediction

To develop a predictive model for BPH, a logistic regression model was constructed using the expression profiles of the two identified biomarkers, PGM2 and GFPT1. The model was used to generate a nomogram for visualizing the contribution of each biomarker in the prediction of disease

status. The nomogram was created using the "rms" R package, which integrates individual biomarker scores into a total predictive score. Additionally, a calibration curve was generated to assess the predictive accuracy and agreement between the predicted and observed probabilities. The study was conducted in accordance with the Declaration of Helsinki and its subsequent amendments.

Results

PIEZO channels are associated with glycometabolic reprogramming and mitochondrial OXPHOS in the progression of BPH

A total of 4,617 DEGs were identified, of which 980 were upregulated and 3,637 were downregulated (*Figure 1A*). These genes reflect significant transcriptional dysregulation in the progression of BPH. Among the DEGs, 122 genes overlapped with the glycolysis and OXPHOS gene sets, forming the differentially expressed glycolysis-OXPHOS subset (*Figure 1B*). This subset represents the intersection of metabolic reprogramming and mitochondrial activity in BPH. The Spearman correlation analysis revealed 84 DE-glycolysis-OXPHOS genes strongly associated with PIEZO1 and PIEZO2 expression ($|Cor| > 0.6$, $P<0.05$). These PIEZO-related genes were visualized in heatmaps and correlation plots, highlighting their relevance to PIEZO channel activity in BPH (*Figure 1C*).

The functional enrichment analysis demonstrated that the PIEZO-related DE-glycolysis-OXPHOS genes were involved in key BPs, including energy derivation via the oxidation of organic compounds and hexose metabolic processes (*Figure 1*, D1). The CC analysis highlighted the mitochondrial matrix and ATPase complexes as major sites of activity (*Figure 1*, D2). The enriched MFs included ATPase activity and proton transmembrane transport (*Figure 1*, D3). The KEGG pathway analysis identified OXPHOS and the tricarboxylic acid (TCA) cycle as critical pathways associated with PIEZO activity and glycometabolic reprogramming in BPH (*Figure 1*, D4).

Identification of biomarkers for BPH progression using logistic regression, protein-protein interaction (PPI) analysis, and machine learning models

The logistic regression analysis identified 21 genes significantly associated with BPH progression ($P<0.05$). These genes were displayed in a forest plot, highlighting their odds ratios and confidence intervals (*Figure 2A*). Among the 21 genes, 12 were found to have significant PPIs. These interactions were visualized in a PPI network, highlighting the functional clusters and pathways associated with glycometabolic reprogramming and mitochondrial activity in BPH (*Figure 2B*).

The random forest model stabilized at 300 decision trees, achieving consistent error reduction (*Figure 2*, C1). Ten genes with the highest Gini coefficient scores were identified as important features and displayed in a feature importance plot, providing insights into their relevance in BPH progression (*Figure 2*, C2). The SVM model achieved its optimal accuracy of 0.92 with six features (*Figure 2D*). By intersecting the biomarkers identified through the random forest and support vector machine (SVM) models, five overlapping genes were identified: *ACAA1*, *GFPT1*, *GNE*, *PGM2*, and *ATP6V1D* (*Figure 2E*). These genes were displayed in a Venn diagram, highlighting their shared significance across machine learning models (*Figure 2E*).

Validation of GFPT1 and PGM2 as robust diagnostic biomarkers for BPH

In the ROC curve analysis, *GFPT1* and *PGM2* achieved AUC values exceeding 0.75 in both the training (GSE132714) and validation datasets (GSE7307 and GSE6099), indicating their strong diagnostic ability to differentiate between the BPH and normal samples (*Figure 3A*). Additionally, the Wilcoxon analysis confirmed that *GFPT1* and *PGM2* were significantly differentially expressed between the BPH and normal samples across all datasets. Their consistent upregulation in the BPH samples supports their role as robust biomarkers for disease progression. These results were displayed in boxplots to compare expression levels (*Figure 3B*).

Immune cell infiltration and its association with PIEZO-associated biomarkers in BPH

The CIBERSORT algorithm revealed distinct immune cell composition profiles between the BPH and normal samples. Stacked bar plots showed the relative abundance of 22 immune cell types across the samples, revealing notable differences in immune cell proportions between the two groups (*Figure 4A*). Wilcoxon rank-sum tests revealed significant differences in the abundance of several immune cell types between the BPH and normal samples. Violin plots showed that specific immune cells, such as macrophages and

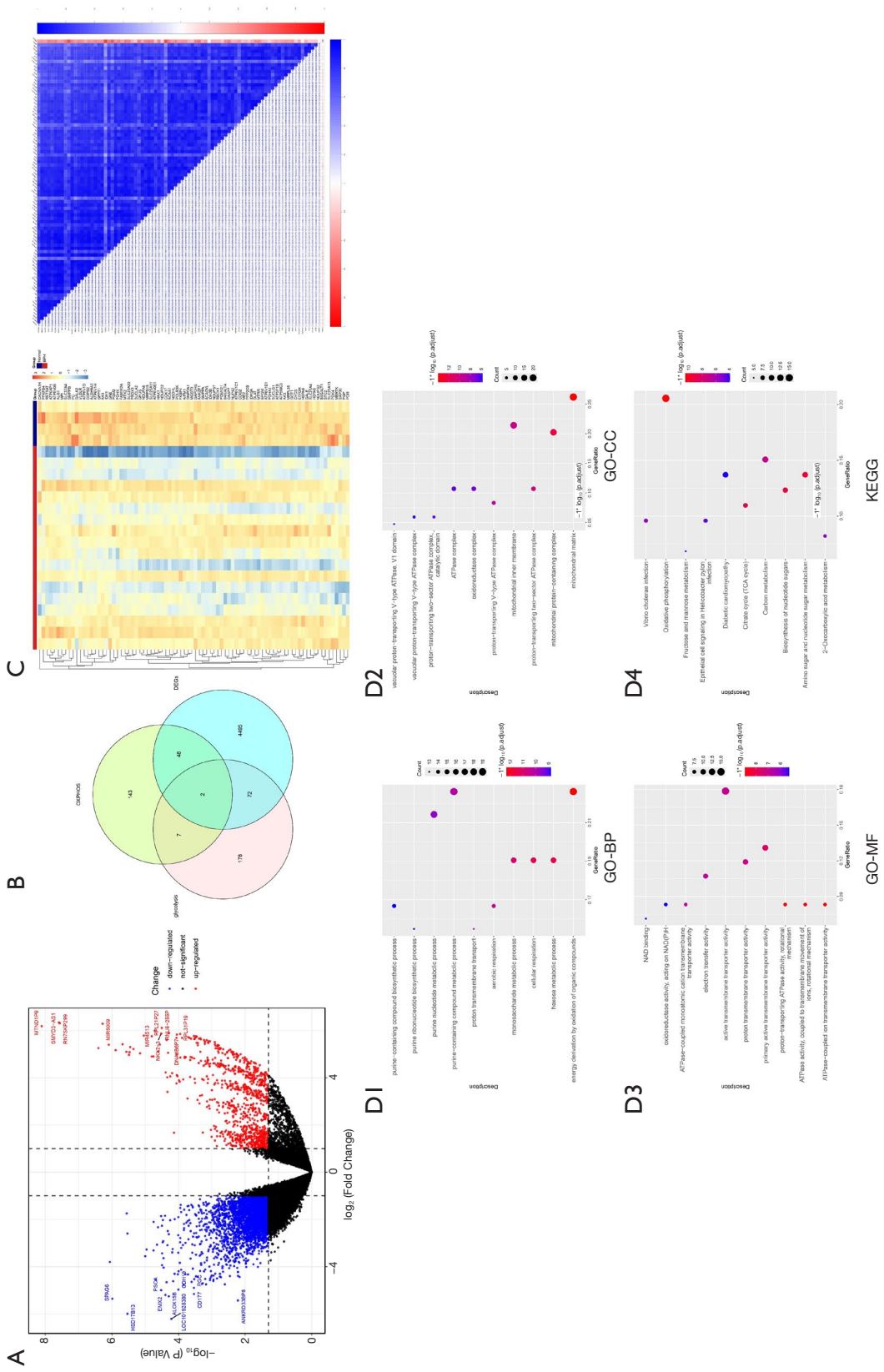

Figure 1 PIEZO channels link glycometabolic reprogramming to OXPHOS in BPH. (A) Volcano plot of DEGs between the BPH and control samples. Genes with a $|\log_2 FC| > 1$ and $P<0.05$ were considered significant. (B) Venn diagram illustrating the overlap between the DEGs and glycolysis/OXPHOS gene sets. The 122 intersecting genes represent the glycometabolic and mitochondrial OXPHOS-related DEGs. (C) Heatmap and correlation plot showing DE-glycolysis-OXPHOS genes strongly correlated with PIEZO1/PIEZO2 expression. Genes with a $|Cor| > 0.6$ and a P value <0.05 were defined as candidate PIEZO-related genes. (D) Enrichment analysis of PIEZO-related glycometabolic and mitochondrial OXPHOS genes. (D1) Top 10 BPs. (D2) Top 10 CCs. (D3) Top 10 MFs. (D4) Top 10 KEGG pathways. BP, biological process; BPH, benign prostatic hyperplasia; CC, cellular component; DEG, differentially expressed gene; FC, fold change; GO, Gene Ontology; KEGG, Kyoto Encyclopedia of Genes and Genomes; MF, molecular function.

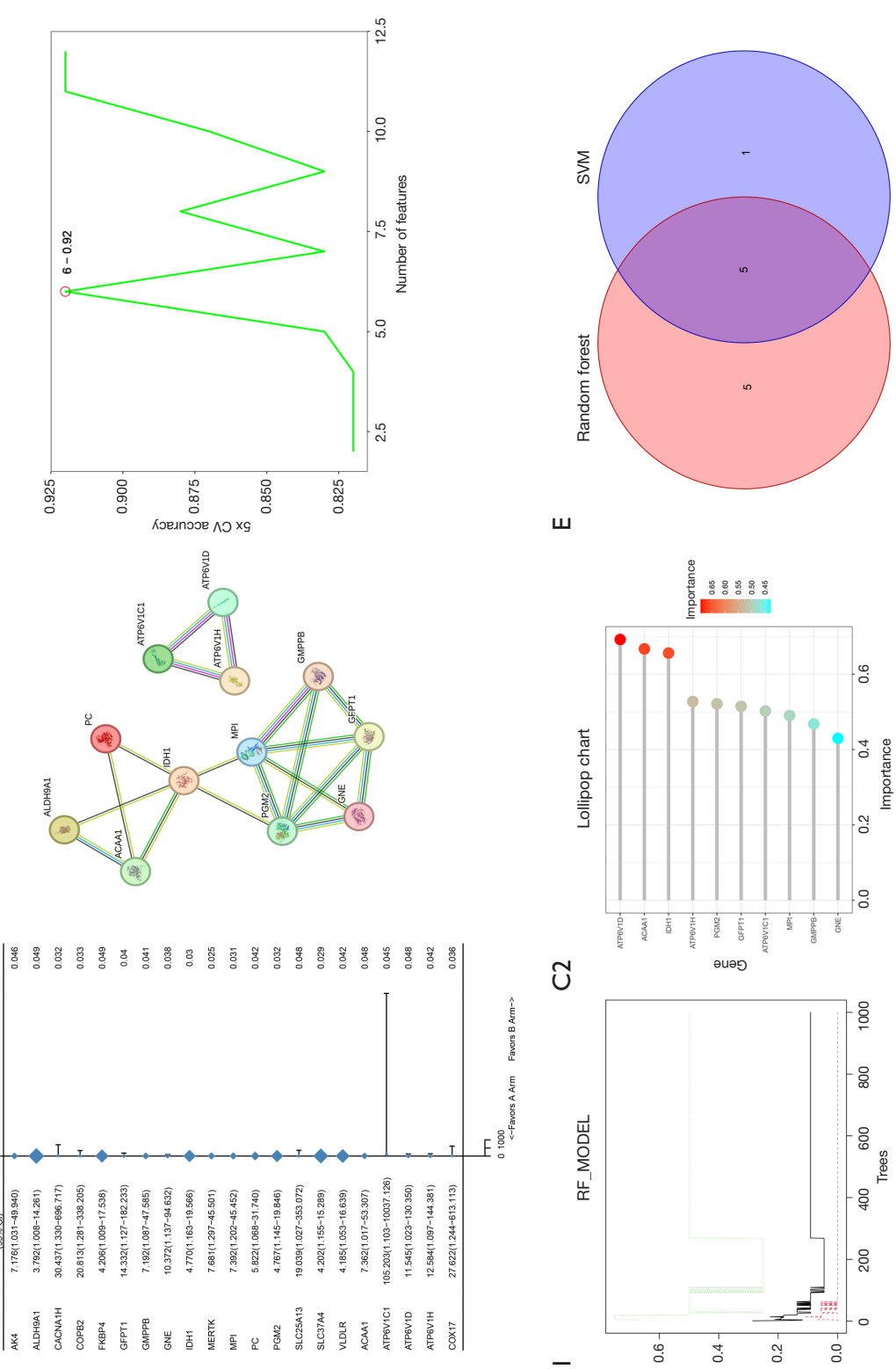

Figure 2 Identification of biomarkers for BPH progression. (A) Forest plot showing the results of the univariate logistic regression analysis of 21 genes significantly associated with BPH progression (P<0.05). (B) PPI network constructed for the 21 candidate genes identified through logistic regression. Twelve genes with significant interactions are shown, highlighting functional clusters and pathways involved in glycometabolic reprogramming and mitochondrial activity. (C) Random forest analysis of the 21 candidate genes. (C1) Relationship between the number of decision trees and model error, demonstrating model stabilization at 300 trees. (C2) Feature importance plot indicating the top 10 genes with the highest Gini coefficient scores, reflecting their relevance in BPH progression. (D) SVM model accuracy as a function of the number of features. (E) Venn diagram illustrating the overlap of biomarkers identified through random forest and SVM models. BPH, benign prostatic hyperplasia; CI, confidence interval; CV, cross-validation; PPI, protein-protein interaction; RF, random forest; SVM, support vector machine.

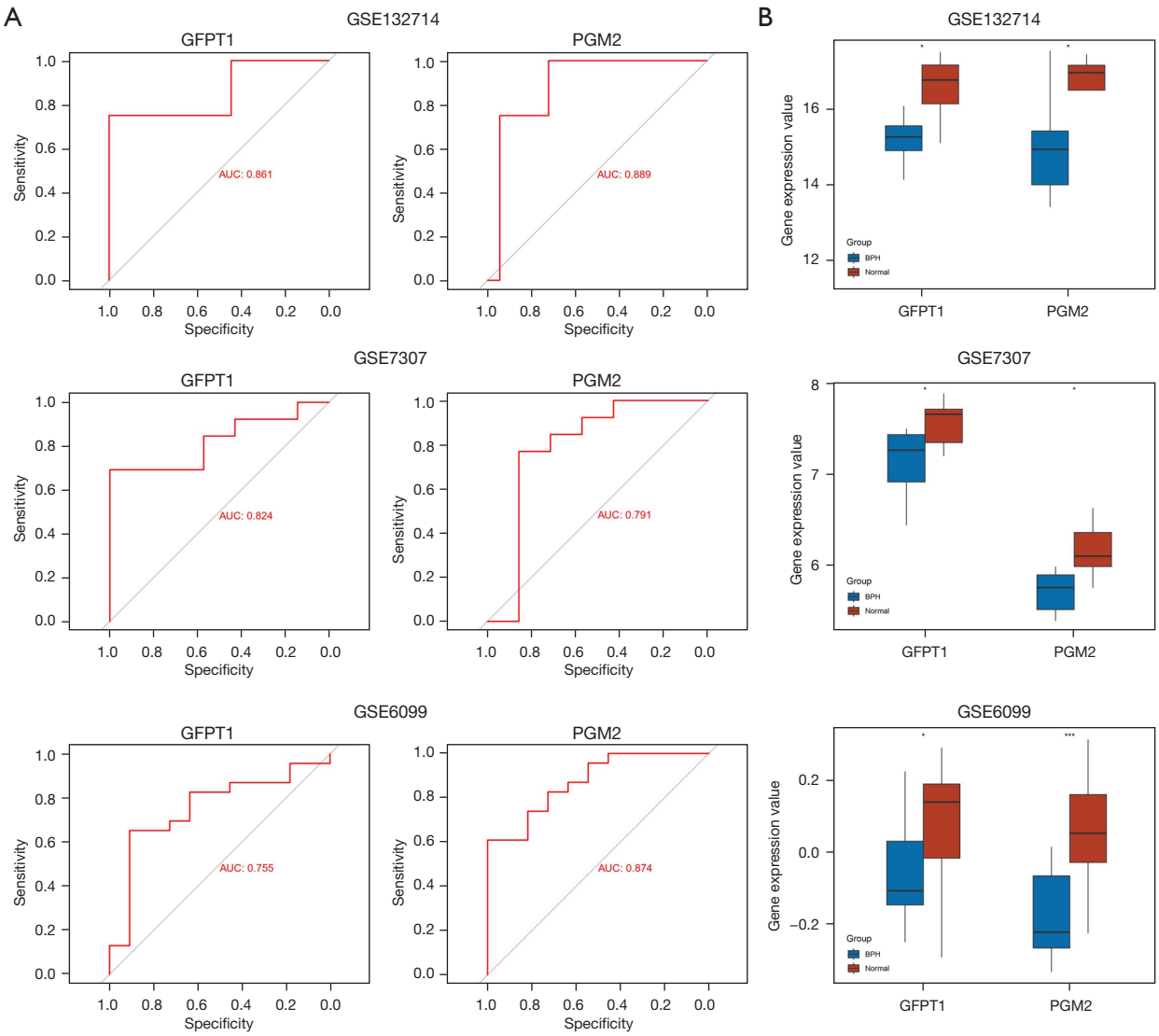

Figure 3 Validation of GFPT1 and PGM2. (A) ROC curves for biomarkers GFPT1 and PGM2 in the training dataset (GSE132714) and validation datasets (GSE7307 and GSE6099). (B) Boxplots comparing the expression levels of GFPT1 and PGM2 between the BPH and normal samples across the training (GSE132714) and validation datasets (GSE7307 and GSE6099). Statistical significance was assessed using the Wilcoxon test, confirming the consistent upregulation of both genes in the BPH samples. *, P<0.05; ***, P<0.001. AUC, area under the curve; BPH, benign prostatic hyperplasia; ROC, receiver operating characteristic.

T-cell subsets, were significantly altered in the BPH samples compared to the control samples, indicating their potential role in disease progression (*Figure 4B*). The Spearman correlation analysis revealed significant associations between the biomarkers *GFPT1* and *PGM2* and several immune cell types in BPH. Notably, the correlations exceeded the threshold of |Cor| >0.3 and were statistically significant (P<0.05). These findings suggest potential interactions between PIEZO-associated biomarkers and immune cell activity in BPH (*Figure 4C*).

Functional pathway enrichment analysis of GFPT1 and PGM2 in BPH

The GSEA revealed that *GFPT1* and *PGM2* were significantly associated with multiple KEGG pathways relevant to glycometabolic reprogramming and mitochondrial activity in BPH. The top six enriched

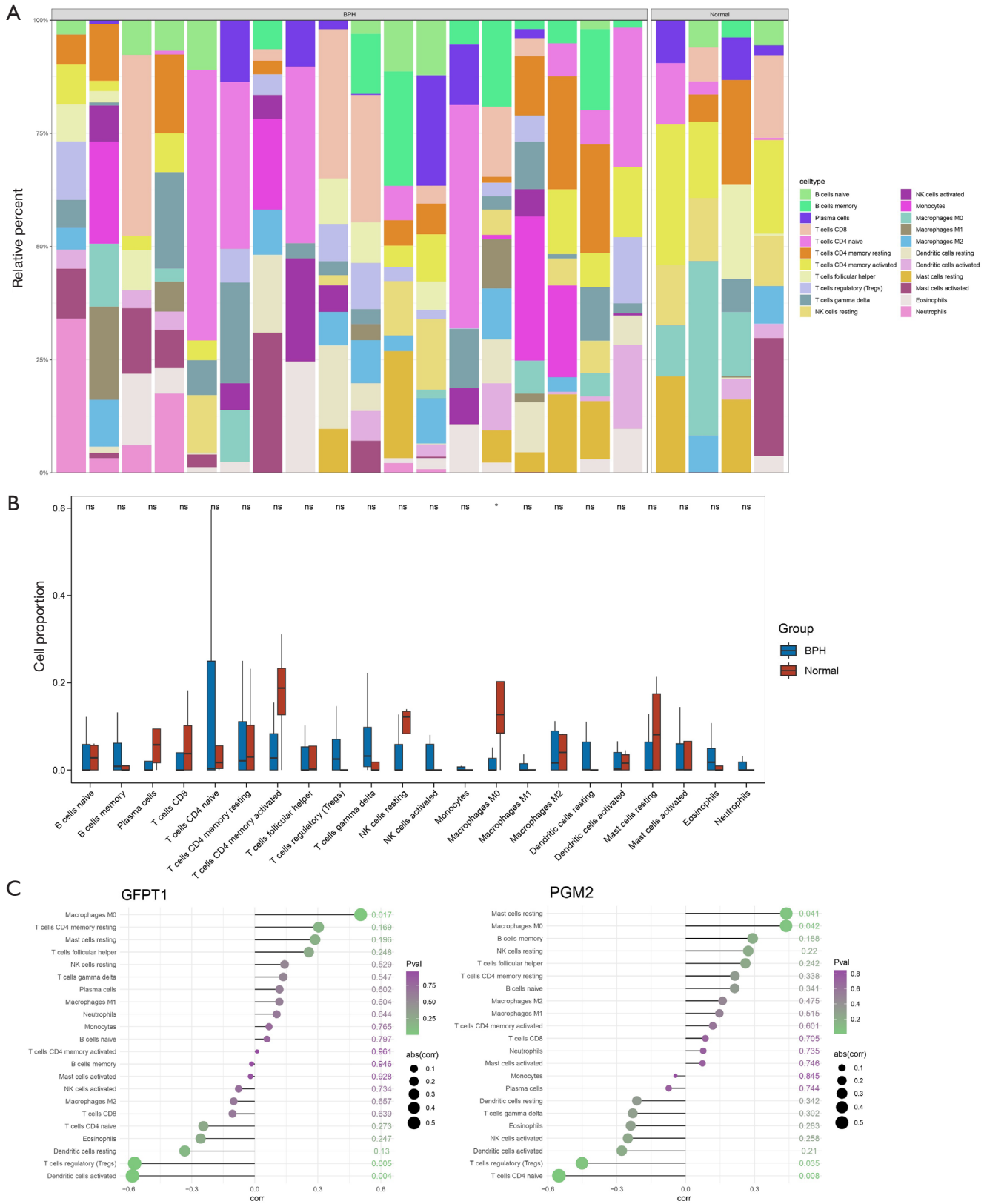

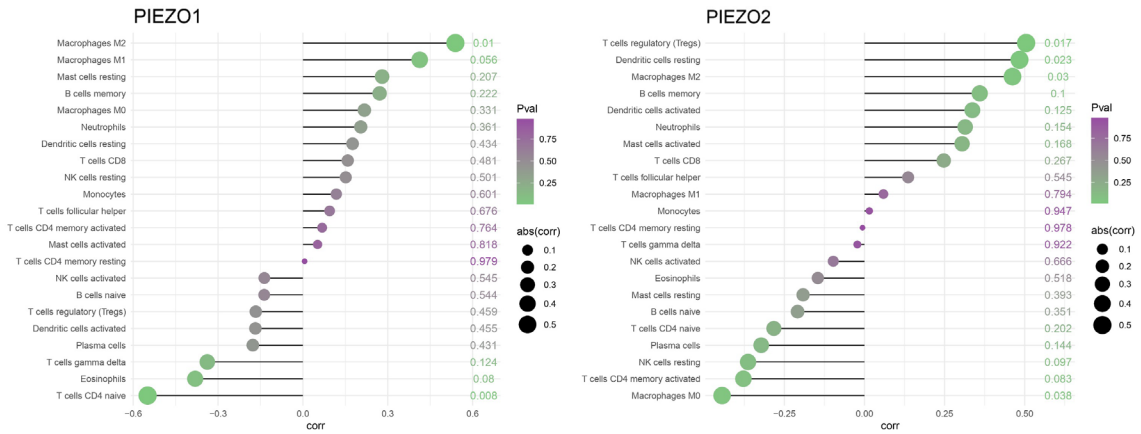

Figure 4 Immune cell infiltration. (A) Stacked bar plot illustrating the relative abundance of 22 immune cell types in the BPH and normal samples, as determined by the CIBERSORT algorithm. Differences in immune cell composition between the two groups are highlighted. (B) Violin plots displaying the differential abundance of 22 immune cell types between the BPH and normal samples. The statistical analysis was performed using Wilcoxon rank-sum tests, showing significant alterations in specific immune cells such as macrophages and T-cell subsets. (C) Lollipop plots showing significant correlations between the biomarkers GFPT1, PGM2, PIEZO1, and PIEZO2 and immune cell infiltration levels in the BPH samples. ns, P>0.05; *, P<0.05. BPH, benign prostatic hyperplasia.

pathways for each hub gene highlighted their involvement in critical cellular processes such as OXPHOS and metabolic regulation (*Figure 5A*). The GSVA revealed distinct pathway activation patterns between high- and low-expression groups for *GFPT1* and *PGM2*. Differentially activated pathways were identified, with pathways with *t* values >0 enriched in the high-expression group and those with *t* values <0 enriched in the low-expression group. These results underscore the functional heterogeneity associated with the expression of these hub genes in BPH (*Figure 5B*).

The ceRNA network of PIEZO and biomarker genes

A ceRNA network was successfully constructed, integrating PIEZO genes (*PIEZO1* and *PIEZO2*), biomarkers (*GFPT1* and *PGM2*), five miRNAs, and 16 lncRNAs. The network comprised 25 nodes and 32 edges, representing complex regulatory relationships among these components. Key miRNAs (e.g., hsa-miR-16-5p and hsa-miR-124-3p) and lncRNAs (e.g., XIST and MALAT1) were highlighted, underscoring their potential roles in regulating glycometabolic reprogramming and mitochondrial activity in the progression of BPH. The network visualization provides insights into the ceRNA-mediated regulatory mechanisms (*Figure 6*).

Nomogram and calibration curve for BPH prediction

A nomogram was constructed based on the logistic regression model using *PGM2* and *GFPT1* expression profiles, enabling the visualization of individual contributions to BPH prediction. The nomogram illustrates the relationship between the biomarker expression levels, total predictive scores, and the probability of disease (*Figure 7A*). The calibration curve analysis showed good agreement between the predicted and observed probabilities, confirming the reliability and clinical utility of the model in predicting BPH status (*Figure 7B*).

Discussion

This study conducted a comprehensive bioinformatics analysis to elucidate the interaction between the PIEZO channels and genes related to glycometabolic reprogramming and mitochondrial OXPHOS in the progression of prostatic hyperplasia. The results provide novel insights into the molecular mechanisms underlying prostatic hyperplasia, which may inform the therapeutic targeting of glycometabolic pathways and PIEZO-mediated signaling.

The interaction between PIEZO channels and metabolic pathways such as glycolysis and OXPHOS is central to

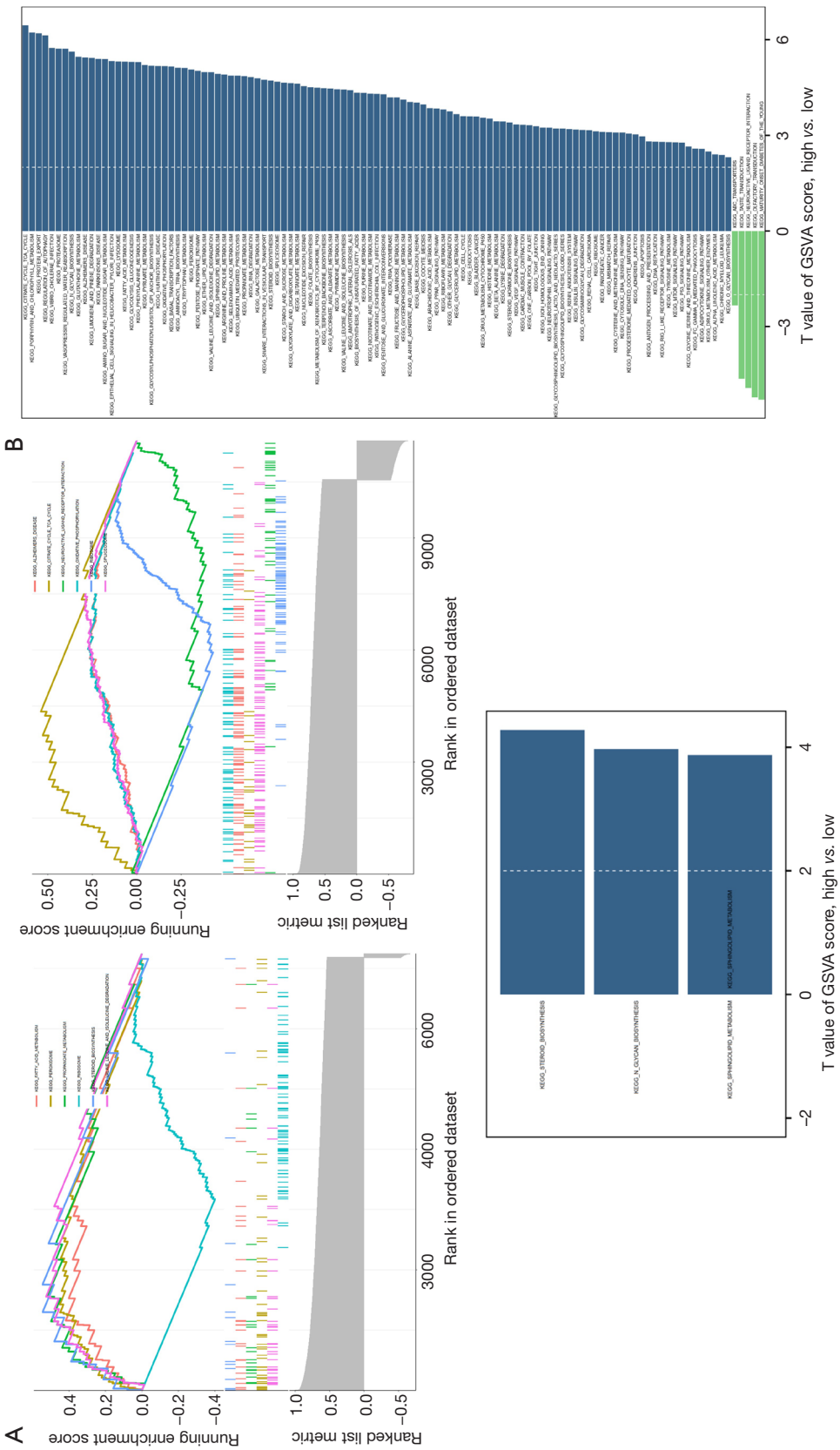

Figure 5 Functional pathway enrichment analysis. (A) Single-sample GSEA results for the hub genes *GFPT1* and *PGM2*. The top six KEGG pathways enriched for each hub gene are shown. (B) GSVA results comparing pathway activation patterns between high- and low-expression groups of *GFPT1* and *PGM2*. GSEA, Gene Set Enrichment Analysis; GSVA, Gene Set Variation Analysis; KEGG, Kyoto Encyclopedia of Genes and Genomes.

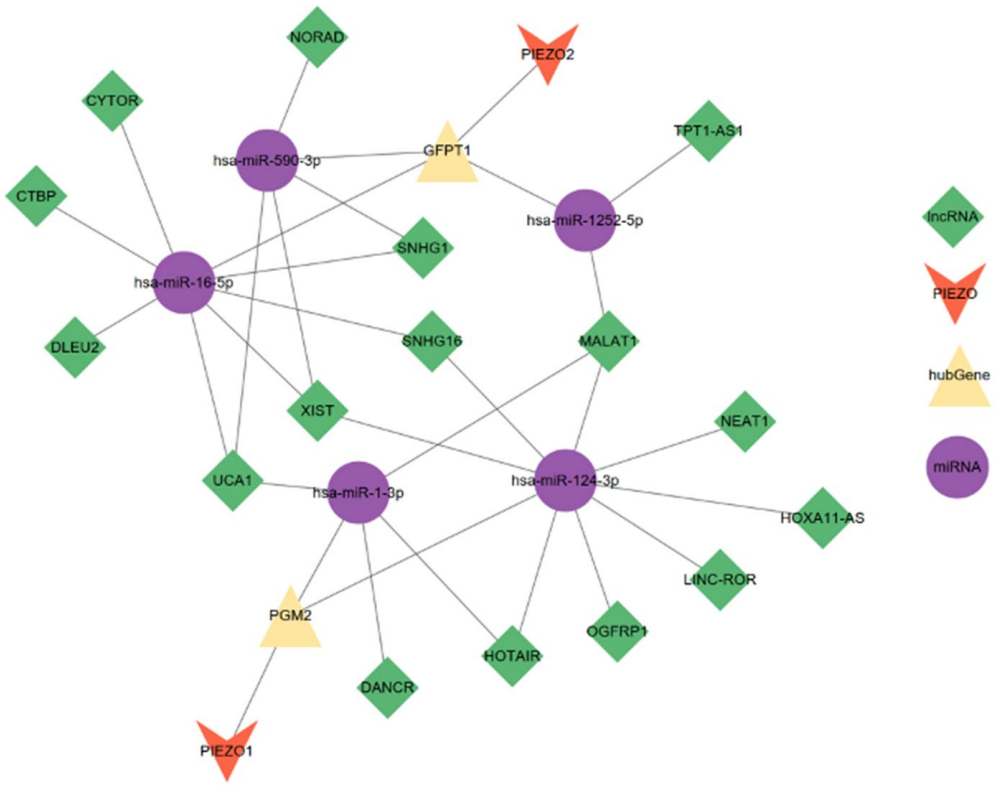

Figure 6 The ceRNA network integrating PIEZO genes (*PIEZO1* and *PIEZO2*), biomarkers (*GFPT1* and *PGM2*), miRNAs, and lncRNAs. The network includes 25 nodes (2 PIEZO genes, 2 biomarkers, 5 miRNAs, and 16 lncRNAs) and 32 edges, illustrating the complex regulatory interactions. Edges indicate experimentally or computationally validated interactions (a score >0.7). ceRNA, competitive endogenous RNA; lncRNA, long non-coding RNA; miRNA, microRNA.

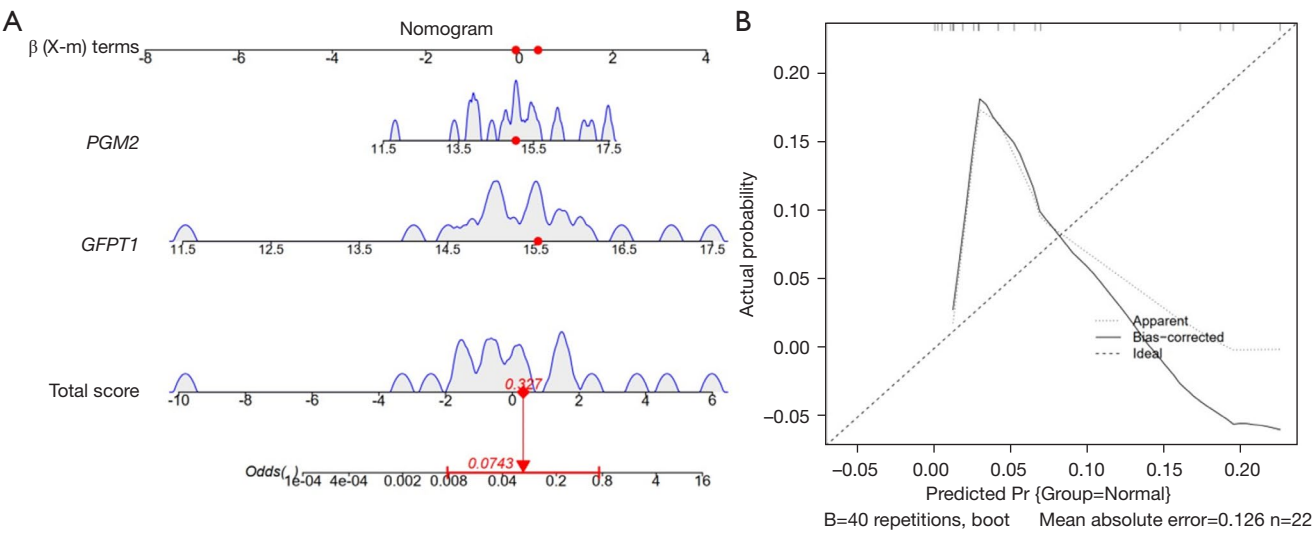

Figure 7 Nomogram and calibration curve. (A) Nomogram constructed from the logistic regression model incorporating the biomarkers *PGM2* and *GFPT1*. The top panel represents individual biomarker contributions, while the bottom panel shows the total predictive score and corresponding odds of disease probability. (B) Calibration curve for the nomogram model. The plot shows the agreement between the predicted (x-axis) and observed (y-axis) probabilities.

understanding cellular energy homeostasis, particularly in the context of prostatic hyperplasia. Recent studies have shown that mechanosensitive ion channels (such as PIEZO1 and PIEZO2) play a critical role in detecting and transducing mechanical stimuli, thereby influencing cell metabolism and behavior (7,14,15). The discovery that these channels can modulate glycometabolic pathways highlights their dual role in mechanotransduction and metabolic regulation, revealing potential therapeutic targets in prostate-related conditions.

PIEZO channels have been implicated in various metabolic processes. For example, PIEZO1 activation has been shown to increase intracellular calcium levels, which can activate the phosphoinositide 3-kinase (PI3K)/Akt pathway—a crucial regulator of metabolic reprogramming (16,17). Elevated Akt signaling is associated with enhanced glycolysis and increased lactate production, reflecting a shift toward aerobic glycolysis, commonly observed in tumor cells under hypoxic conditions (18,19). This phenomenon, also known as the Warburg effect (20), is a key metabolic alteration observed in hyperplastic and cancerous tissues, facilitating rapid cell proliferation and survival in unfavorable microenvironments. Moreover, research suggests that PIEZO1 activation may enhance mitochondrial respiration and ATP production, further linking mechanosensation to mitochondrial function (19,21).

In prostate cells, where energetic demands are typically elevated during hyperplastic growth, the interplay between PIEZO channels and OXPHOS pathways could serve as a compensatory mechanism to meet increased bioenergetic needs. The dysregulation of these pathways can lead to metabolic inflexibility, whereby cells become overly reliant on glycolytic metabolism, thus contributing to the pathology of BPH and possibly the progression of cancer (18,22).

The role of PIEZO channels as mediators of mechanical forces affecting metastatic potential has also attracted attention. Tumors are subjected to mechanical stresses due to the surrounding extracellular matrix and tissue architecture. The ability of PIEZO channels to transduce these mechanosensory signals and subsequently recalibrate metabolic activities emphasizes their role in tumor microenvironment adaptation. For example, increased PIEZO1 expression in prostate carcinoma tissues is correlated with increased cell migration and proliferation, implicating its role in tumor aggressiveness (23,24). In this context, the chronic activation of PIEZO channels may promote sustained glycolytic activity while impairing mitochondrial function, resulting in a metabolic state that favors hyperplastic growth (25).

Based on the successfully constructed ceRNA network integrating PIEZO1/2, we propose to screen for core regulatory axes using a topological prioritization approach combined with functional enrichment analysis. From this framework, three experimentally testable hypotheses emerge: (I) the lncRNA MALAT1 acts as a ceRNA for hsa-miR-16-5p, relieving inhibition of GFPT1 expression, thereby enhancing hexosamine biosynthesis pathway flux to support glycosylation and proliferation in PIEZO-activated hyperplastic cells; (II) XIST sponges hsa-miR-124-3p to upregulate PGM2, promoting glycolysis by increasing glucose-6-phosphate utilization, establishing a PIEZO2-mediated mechano-metabolic axis in BPH progression; and (III) a PIEZO1/hsa-miR-16-5p/GFPT1 regulatory loop exists wherein mechanical stimulation downregulates this miRNA to coordinately upregulate both glycolytic (PGM2) and hexosamine (GFPT1) pathway genes, which can be validated by treating BPH-derived stromal cells with PIEZO agonist Yoda1 or siRNA targeting these ncRNAs, followed by Seahorse metabolic flux analysis and measurement of UDP-GlcNAc levels as functional readouts.

GFPT1 and PGM2 are metabolic enzymes with established but incompletely characterized roles in BPH. GFPT1 is the rate-limiting enzyme of the hexosamine biosynthesis pathway (HBP), generating UDP-N-acetylglucosamine for protein glycosylation, and its upregulation in BPH has been linked to TGF-β1-induced extracellular matrix deposition and stromal remodeling. PGM2 catalyzes the interconversion of glucose-1-phosphate and glucose-6-phosphate, channeling glucose intermediates toward glycogen synthesis and glycolysis to support the biosynthetic demands of proliferating stromal and epithelial cells. ROC and Wilcoxon analyses consistently demonstrate that both genes are significantly upregulated in BPH samples compared to normal prostate tissue across multiple independent datasets (GSE132714, GSE7307, GSE6099), confirming their robust differential expression. Regarding colocalization with PIEZO channels, while direct immunohistochemical evidence in BPH tissue remains unreported, correlation analysis revealing 84 PIEZO-associated metabolic genes and the constructed ceRNA network linking PIEZO1/2 to GFPT1 and PGM2 via shared miRNAs strongly suggests coordinated regulation. Mechanistically, PIEZO-mediated calcium influx can activate NF-κB and HIF-1α—transcription factors with predicted binding sites on the GFPT1 and PGM2 promoters—while PIEZO-driven PI3K/Akt signaling may

enhance their expression via mTOR-mediated regulation of CREB and SREBP1. Thus, we hypothesize that in mechanically stressed regions of hyperplastic prostate tissue, PIEZO activation locally upregulates GFPT1 and PGM2 to meet increased metabolic and glycosylation demands, a mechanism warranting validation through immunohistochemical colocalization studies and PIEZO agonist/antagonist experiments in BPH-derived cell models.

Recent studies suggest that PIEZO channels play a complex regulatory role in coupling mechanotransduction with metabolic reprogramming. Their involvement in glycolytic and OXPHOS pathways not only provides insights into the metabolic landscapes of hyperplastic prostatic cells but also reveals therapeutic opportunities to target these pathways. Potential interventions leveraging PIEZO channel modulation may restore metabolic balance and disrupt the hyperplastic phenotype, offering a promising avenue for future research and clinical applications in prostate health.

The significant correlations observed between PIEZO channel expression and the dysregulation of key glycolysis- and OXPHOS-related genes underscore the potential role of these channels as critical mediators in metabolic pathways associated with prostatic hyperplasia. Recent studies have highlighted the intricate relationship between mechanotransduction and metabolic regulation, suggesting that PIEZO channels may essentially function as upstream regulators in the process of metabolic reprogramming in BPH (26). Mechanically activated ion channels, particularly PIEZO1 and PIEZO2, have been shown to respond to physical stimuli in the microenvironment of cells, which in turn influence various signaling pathways related to metabolism (27). Notably, the mechanosensitive nature of these channels allows them to react swiftly to changes in tissue tension and pressure, typical of the pathophysiological conditions present in BPH. Such activation can trigger downstream effects that alter energy production pathways, primarily through glycolysis and OXPHOS, which are key metabolic processes in rapidly proliferating tissues (28).

Studying the interplay between mechanical stress and metabolic pathways could advance our understanding of BPH. For example, the activation of PIEZO channels has been reported to influence intracellular calcium levels, which are crucial for regulating various enzymes involved in glycolysis and the TCA cycle (29,30). Research has shown that elevated intracellular calcium can enhance glycolytic flux to support the energy demands of hypertrophied prostatic tissues (31). This metabolic shift not only facilitates continuous cell proliferation but also promotes survival under stress conditions by favoring anaerobic glycolysis, known as the Warburg effect.

The dysregulation of hallmark genes associated with glycolysis and OXPHOS could also advance our understanding of BPH progression. Enhanced expression of glycolytic enzymes, such as hexokinase and lactate dehydrogenase, along with alterations in OXPHOS components, suggests that these metabolic pathways are crucial determinants of the cellular phenotypes observed in hyperplastic prostate tissue. By linking the mechanical signals received via PIEZO channels to metabolic changes, we can appreciate how altered mechanotransduction could lead to an epigenetic landscape favoring aggressive proliferation and poorer clinical outcomes in BPH patients.

Additionally, the targeting of PIEZO channels offers an exciting prospect for novel interventions in the management of BPH. The pharmacological modulation of PIEZO channel activity or downstream metabolic pathways could potentially ameliorate the dysregulated metabolic profile observed in this condition, offering a new option for treatment strategies. Research focused on developing selective PIEZO channel modulators could not only clarify their role in tumor metabolism but could also provide insights into the broader context of mechanobiology in cancer progression.

The integration of multi-cohort data from the GEO datasets was invaluable in validating our findings across a variety of biological samples, including serum, mucosa, and tissue. This method not only enhanced the robustness of our results but also provided a comprehensive perspective on the implications of PIEZO signaling in diverse tissue environments. The ability to replicate findings across different biological samples bolsters the credibility of our interpretations and suggests that PIEZO channels play a significant role in modulating biological responses across various contexts.

PIEZO proteins respond to physical stimuli; the resulting increase in intracellular Ca^{2+} serves as a pivotal second messenger that initiates several downstream signaling cascades directly linked to metabolic regulation (9). Concurrently, PIEZO-mediated Ca^{2+} signaling can activate the PI3K/Akt pathway, a central hub for promoting aerobic glycolysis and cell survival, while also influencing mitochondrial OXPHOS by potentially modulating mitochondrial calcium uptake and respiration, though the precise mechanisms linking PIEZO to mitochondrial function are still under investigation (22). Furthermore,

PIEZO1 activation has been shown to influence the MAPK/ERK signaling pathway and induce the expression of vascular endothelial growth factor (VEGF), linking mechanotransduction not only to metabolic adaptation but also to angiogenesis and cell proliferation in response to environmental cues (29).

Recent research has reported that PIEZO channels are crucial in transducing mechanical stimuli into biochemical signals, thereby influencing cellular behaviors related to cancer progression, including proliferation and migration (6). The mechanotransductive properties of PIEZO proteins lead to a cascade of cellular responses that can alter metabolic pathways, emphasizing their role beyond traditional ion channel functions. Research has shown that PIEZO1 activation can promote the expression of factors involved in angiogenesis, such as HIF-1α, thereby enhancing nutrient supply to tumors and facilitating their growth in hyperplastic conditions (32,33). This connection underscores the dual role of PIEZO in both mechanical signaling and metabolic adaptation.

Our integrated framework advances a unified model wherein PIEZO-mediated mechanotransduction orchestrates metabolic gene expression, immune remodeling, and non-coding RNA regulation—positioning the PIEZO-GFPT1/PGM2 axis as a central hub linking physical forces to the metabolic phenotype of BPH. Our findings also align with observations from various studies indicating that PIEZO channels are implicated in mechanosensitive ion channelopathies contributing to tumorigenesis (34). The current understanding of PIEZO signaling pathways extends to metabolic regulation, particularly under conditions of increased mechanical stress, which is prevalent in the tumor microenvironment (35). Enhanced PIEZO signaling in cancer cells has been associated with metabolic reprogramming, guiding the switch from OXPHOS to glycolytic pathways—often referred to as the Warburg effect. This switch is particularly evident in rapidly proliferating tumors that require substantial energy supply for their growth and survival.

Moreover, the tissue-specific metabolic alterations observed in our analyses suggest that PIEZO channels may play a pivotal role in modulating localized cellular environments, adapting to the unique mechanical and chemical cues presented within different tissues. For example, the activation of PIEZO1 and the subsequent calcium influx not only facilitate cell motility but also trigger metabolic pathways that enhance cancer cell invasiveness and survival (36). This highlights the potential of PIEZO channels as therapeutic targets, where modulation of their activity could exert significant effects on tumor growth and metastasis.

Despite the strengths of our bioinformatics approach, several limitations should be acknowledged. First, the reliance on publicly available datasets introduces variability in sample quality, experimental conditions, and annotation consistency. Although this limitation was mitigated by rigorous preprocessing and cross-validation, experimental heterogeneity remains a potential confounder. Second, our findings were based on in silico analyses and require experimental validation to confirm the functional relevance of PIEZO-glycometabolic interactions. Techniques such as clustered regularly interspaced short palindromic repeats-mediated gene editing, metabolic flux analysis, and PIEZO-specific pharmacological modulation in cell and animal models would be valuable in corroborating our results. Third, the scope of this study was limited to glycolysis and OXPHOS pathways. While these pathways represent critical aspects of cellular metabolism, other metabolic processes, such as lipid metabolism and amino acid biosynthesis, may also contribute to prostatic hyperplasia and merit further exploration.

Building on our findings, future research should prioritize the following directions:

(I) Mechanistic validation: experimental studies are needed to examine the molecular mechanisms by which PIEZO channels regulate glycolytic and mitochondrial pathways. Investigating the role of PIEZO-mediated calcium signaling in these processes would provide mechanistic insights.

(II) Therapeutic targeting: given the critical role of metabolic reprogramming in prostatic hyperplasia, the development of small-molecule inhibitors or modulators targeting PIEZO channels represents a promising therapeutic strategy. Moreover, combining PIEZO modulation with metabolic inhibitors could synergistically suppress hyperplastic growth.

(III) Expanded metabolic profiling: future studies should extend the scope of metabolic analysis to include other pathways, such as lipid and amino acid metabolism, to obtain a more comprehensive understanding of metabolic dysregulation in BPH.

(IV) Clinical relevance: translational studies investigating PIEZO channel expression and metabolic profiles in clinical BPH samples could validate the clinical applicability of our findings and identify potential biomarkers for disease diagnosis and progression.

Conclusions

In conclusion, this study identifies significant correlations between PIEZO channels, glycometabolic genes, immune infiltration, and a ceRNA network in BPH, generating testable hypotheses regarding a potential mechano-metabolic axis. While GFPT1 and PGM2 demonstrate diagnostic utility, the proposed regulatory mechanisms and therapeutic implications remain correlative and require experimental validation through functional studies, including PIEZO modulation in BPH models and verification of predicted ceRNA interactions.

Acknowledgments

None.

Footnote

Reporting Checklist: The authors have completed the TRIPOD reporting checklist. Available at https://tau.amegroups.com/article/view/10.21037/tau-2026-1-0075/rc

Peer Review File: Available at https://tau.amegroups.com/article/view/10.21037/tau-2026-1-0075/prf

Funding: None.

Conflicts of Interest: All authors have completed the ICMJE uniform disclosure form (available at https://tau.amegroups.com/article/view/10.21037/tau-2026-1-0075/coif). The authors have no conflicts of interest to declare.

Ethical Statement: The authors are accountable for all aspects of the work in ensuring that questions related to the accuracy or integrity of any part of the work are appropriately investigated and resolved. The study was conducted in accordance with the Declaration of Helsinki and its subsequent amendments.

References

1. Devlin CM, Simms MS, Maitland NJ. Benign prostatic hyperplasia - what do we know? BJU Int 2021;127:389-99.
2. Miernik A, Gratzke C. Current Treatment for Benign Prostatic Hyperplasia. Dtsch Arztebl Int 2020;117:843-54.
3. Orlov YL, Anashkina AA, Klimontov VV, et al. Medical Genetics, Genomics and Bioinformatics Aid in Understanding Molecular Mechanisms of Human Diseases. Int J Mol Sci 2021;22:9962.
4. Zhou Y, Wang W, Gu H, et al. Buzhongyiqi granules in ulcerative colitis Therapy: Integrated chemical composition, pharmacodynamic validation, and IL-6/STAT3 axis regulation. J Ethnopharmacol 2025;351:120083.
5. Tadge T, Pattewar A, More N, et al. The role of Piezo1 and Piezo2 proteins in tissue engineering: A comprehensive review. Eng Regen 2024;5:170-85.
6. Karska J, Kowalski S, Saczko J, et al. Mechanosensitive Ion Channels and Their Role in Cancer Cells. Membranes (Basel) 2023;13:167.
7. Zhao F, Zhang L, Wei M, et al. Mechanosensitive Ion Channel PIEZO1 Signaling in the Hall-Marks of Cancer: Structure and Functions. Cancers (Basel) 2022;14:4955.
8. Nalongo Bina K. Metabolic reprogramming in prostate cancer: A potential therapeutic target. INOSR Exp Sci 2024;13:15-9.
9. Tan J, Xu Q, Pandupuspitasari NS, et al. Non-coding RNAs-glycolysis axis in cancer therapy resistance: Insight into mechanism to therapeutic solution. Biochem Pharmacol 2025;242:117286.
10. Zhou W, Yin X, Huang J, et al. Verapamil modulates astrocytic glycolytic dysfunction via TXNIP inhibition in the hippocampus of 3 × Tg-AD mice. Biochem Pharmacol 2025;242:117233.
11. Li J, Yang C, Zheng Y. A novel disulfidptosis and glycolysis related risk score signature for prediction of prognosis and ICI therapeutic responsiveness in colorectal cancer. Sci Rep 2023;13:13344.
12. Chen W, Yang Z, Chen Y. A Novel Oxidative Phosphorylation-Associated Gene Signature for Prognosis Prediction in Patients with Hepatocellular Carcinoma. Dis Markers 2022;2022:3594901.
13. Jia Z, Zhang J, Li Z, et al. Identification of ferroptosis-related genes associated with diffuse large B-cell lymphoma via bioinformatics and machine learning approaches. Int J Biol Macromol 2024;282:137117.
14. Qin L, He T, Chen S, et al. Roles of mechanosensitive channel Piezo1/2 proteins in skeleton and other tissues.

Bone Res 2021;9:44.
15. Lin Y, Ren J, McGrath C. Mechanosensitive Piezo1 and Piezo2 ion channels in craniofacial development and dentistry: Recent advances and prospects. Front Physiol 2022;13:1039714.
16. Liu H, Hu J, Zheng Q, et al. Piezo1 Channels as Force Sensors in Mechanical Force-Related Chronic Inflammation. Front Immunol 2022;13:816149.
17. Zhou ZY, Bai N, Zheng WJ, et al. MultiOmics analysis of metabolic dysregulation and immune features in breast cancer. Int Immunopharmacol 2025;152:114376.
18. Han Y, Liu C, Zhang D, et al. Mechanosensitive ion channel Piezo1 promotes prostate cancer development through the activation of the Akt/mTOR pathway and acceleration of cell cycle. Int J Oncol 2019;55:629-44.
19. Jiang M, Zhang YX, Bu WJ, et al. Piezo1 channel activation stimulates ATP production through enhancing mitochondrial respiration and glycolysis in vascular endothelial cells. Br J Pharmacol 2023;180:1862-77.
20. Wang Y, Patti GJ. The Warburg effect: a signature of mitochondrial overload. Trends Cell Biol 2023;33:1014-20.
21. Li X, Kordsmeier J, Nookaew I, et al. Piezo1 stimulates mitochondrial function via cAMP signaling. FASEB J 2022;36:e22519.
22. Wei P, Lin D, Luo C, et al. High glucose promotes benign prostatic hyperplasia by downregulating PDK4 expression. Sci Rep 2023;13:17910.
23. De Felice D, Alaimo A. Mechanosensitive Piezo Channels in Cancer: Focus on altered Calcium Signaling in Cancer Cells and in Tumor Progression. Cancers (Basel) 2020;12:1780.
24. Lopez-Cavestany M, Hahn SB, Hope JM, et al. Matrix stiffness induces epithelial-to-mesenchymal transition via Piezo1-regulated calcium flux in prostate cancer cells. iScience 2023;26:106275.
25. Perin M, Chinigò G, Genova T, et al. The Impact of Plasma Membrane Ion Channels on Bone Remodeling in Response to Mechanical Stress, Oxidative Imbalance, and Acidosis. Antioxidants (Basel) 2023;12:689.
26. Li X, Hu J, Zhao X, et al. Piezo channels in the urinary system. Exp Mol Med 2022;54:697-710.
27. Xiao B. Mechanisms of mechanotransduction and physiological roles of PIEZO channels. Nat Rev Mol Cell Biol 2024;25:886-903.
28. Schiliro C, Firestein BL. Mechanisms of Metabolic Reprogramming in Cancer Cells Supporting Enhanced Growth and Proliferation. Cells 2021;10:1056.
29. Shan F, Zhang N, Yao X, et al. Mechanosensitive channel of large conductance enhances the mechanical stretching-induced upregulation of glycolysis and oxidative metabolism in Schwann cells. Cell Commun Signal 2024;22:93.
30. Zhang X, Leng S, Liu X, et al. Ion channel Piezo1 activation aggravates the endothelial dysfunction under a high glucose environment. Cardiovasc Diabetol 2024;23:150.
31. Zhang Y, Zhang C, Feng R, et al. CXCR4 regulates macrophage M1 polarization by altering glycolysis to promote prostate fibrosis. Cell Commun Signal 2024;22:456.
32. Zhang X, Al-Danakh A, Zhu X, et al. Insights into the mechanisms, regulation, and therapeutic implications of extracellular matrix stiffness in cancer. Bioeng Transl Med 2025;10:e10698.
33. Li R, Liu K, Huang X, et al. Bioactive Materials Promote Wound Healing through Modulation of Cell Behaviors. Adv Sci (Weinh) 2022;9:e2105152.
34. Syeda R. Physiology and Pathophysiology of Mechanically Activated PIEZO Channels. Annu Rev Neurosci 2021;44:383-402.
35. Yu JL, Liao HY. Piezo-type mechanosensitive ion channel component 1 (Piezo1) in human cancer. Biomed Pharmacother 2021;140:111692.
36. Kim YJ, Hyun J. Mechanosensitive ion channels in apoptosis and ferroptosis: focusing on the role of Piezo1. BMB Rep 2023;56:145-52.

Cite this article as: Zheng Y, Zhao F, Xu P, Zeng C, Sun Z, Wu G, Wang Y. A bioinformatics analysis of the PIEZO channel interaction network and the genes related to glycometabolic reprogramming and mitochondrial oxidative phosphorylation in the progression of prostatic hyperplasia. Transl Androl Urol 2026;15(4):131. doi: 10.21037/tau-2026-1-0075

